Diyala Journal of Engineering Sciences

Journal homepage: https://djes.info/index.php/djes

ISSN: 1999-8716 (Print); 2616-6909 (Online)

Incorporation of Spiral fins for improvement of discharging rate in Latent Heat Storage Unit

Digant S. Mehta[1,2 *], Manish K. Rathod[3], Jyotirmay Banerjee[3]

[1] Mechanical Engineering Department, Government Engineering College, Palanpur, Gujarat, India.
[2]Gujarat Technological University, Ahmedabad, Gujarat, India.
[3]Department of Mechanical Engineering, S.V.National Institute of Technology, Surat, India.

ARTICLE INFO

Article history:
Received 26/05/2025.
Revised 30/09/2025.
Accepted 12/10/2025.
Available online 10/12/2025.

Keywords:
Latent Heat Storage Unit (LHSU)
Shell and Tube
Phase Change Material (PCM)
Spiral fins
Discharging

ABSTRACT

Latent Heat Storage Units (LHSUs) are widely used for low-temperature thermal applications, but their energy retrieval rate during solidification is restricted by the low thermal conductivity of most phase change materials (PCMs). Enhancing heat transfer during discharging is therefore essential for improving system efficiency and enabling practical solar thermal integration. This study experimentally evaluates the effectiveness of spiral fins in augmenting the discharging rate of a shell-and-tube LHSU filled with stearic acid as PCM and water as the heat transfer fluid (HTF). A custom-developed test rig with adjustable orientation (vertical, horizontal, and inclined) was fabricated, and temperature measurements were captured using 45 K-type thermocouples distributed over five axial planes within the annular PCM region. Discharging experiments were performed at an HTF inlet temperature of 28 °C and 5 LPM flow rate. The results confirm that spiral fins substantially accelerate solidification, reducing the time required to reach an average PCM temperature of 35 °C by 26.5%, 25.96% and 24.37% at the middle section for vertical, horizontal, and inclined orientations, respectively. For the entire annulus, the reduction ranged from 17.2% to 19.58%, demonstrating orientation-independent enhancement. The dominance of conduction during solidification minimizes buoyancy-driven convective effects, making spiral fins a reliable design feature for practical installations irrespective of mounting angle. The findings validate spiral fins as a robust heat transfer enhancement method for LHSUs and provide experimental insights for system optimization in real-world thermal energy storage applications.

1. INTRODUCTION

For developing countries like India, technological advancements in renewable energy are essential to meet rising energy demands. One of the potential source of renewable energy is Solar thermal energy which can be incorporated to meet the energy demand in industrial and residential sectors. Solar thermal energy sector has significant applications in heating and cooling of the buildings [1, 2]. Thermal Energy storage plays a crucial role in the stabilization and balancing of electrical grids. It acts as a safeguard against the irregular nature of solar energy. Storage of thermal energy can be executed by Phase Change Materials (PCMs) which change phase during the energy storage/retrieval process. Such processes of energy storage and retrieval are referred as melting (charging) and solidification (discharging) respectively. Latent heat storage is an attractive method for thermal energy storage due to its nearly isothermal phase change process and high energy density. However, its effectiveness is often limited by the low thermal conductivity (0.15 – 0.3 W/m·K) of most phase change materials (PCMs) [3, 4]. Hence, use of LHSU is restricted in real life solar thermal applications due to impediment in charging and discharging time. Moreover, charging and discharging phenomena is significantly affected by containers known as Latent Heat Storage Units (LHSUs) in which PCMs are accumulated. Ding et al. [5] revealed that shell-and-tube LHSU exhibits greater performance in terms of charging and discharging cycle as compared to rectangular and cylindrical LHSUs.

With the above background, enhancing the performance of shell-and-tube LHSUs - particularly by reducing PCM charging and discharging time is crucial for making them more viable in practical solar thermal applications. Influence of orientation also

*Corresponding author's Email: dsm@gecpalanpur.ac.in
DOI: 10.24237/djes.2025.18403

affects the heat transfer mechanisms (conduction and convection) which direct the rate of charging and discharging of PCM [6-7]. Heat transfer mechanisms during charging and discharging are sometimes depend on parameter like HTF temperature and HTF mass flow rate along with different HTF tube size. Aljumaily et al. [8] study combined experiments and ANSYS simulations to assess the impact of mass flow rates (2 and 4 L/min) and tube geometries on PCM solidification in a shell-and-tube heat exchanger. Results show that circular tubes achieve the highest thermal efficiency (≈71.6%), with heat transfer shifting from convection to conduction as solidification progresses. Aljumaily et al. [9] has investigated PCM solidification in a shell-and-tube exchanger at 2 L/min, comparing circular and elliptical tube shapes through experiments and CFD. The circular tube showed superior performance, achieving up to 71.6% efficiency, confirming geometry's strong influence on heat transfer. Aljumaily et al. [10] has carried out a comparative analysis of different inner tube geometries on the performance of a shell-and-tube Latent Heat Thermal Energy Storage system. The authors effectively combine experimental and 3D numerical approaches to demonstrate that a circular inner tube configuration yields superior heat transfer and energy storage efficiency compared to other polygonal and elliptical shapes.

The charging and discharging performance of latent heat storage systems can be enhanced by improving heat transfer rates through various thermal conductivity enhancement techniques. These include the integration of fins, metal foam matrices, nanoparticles, micro/macro encapsulation, and the use of multiple PCMs [11,12]. However, heat transfer enhancement in LHSU using fins represents best alternative compared to other techniques due to lesser cost, simple structure and easy in fabrication. Niyas et al. [13] paper experimentally investigates a lab-scale latent heat storage prototype using a shell-and-tube heat exchanger with finned tubes and a ternary salt mixture as PCM. It demonstrates that charging is convection-enhanced and faster than discharging, achieving ~16.9 MJ storage and ~15.4 MJ recovery, with performance strongly influenced by HTF inlet temperature and flow rate

Many researchers have conducted experimental and numerical investigations to improve the thermal cycling rate of LHSUs, exploring fin types such as annular, longitudinal, and helical/spiral. Several authors have incorporated annular fins [14-20] and longitudinal fins [21-30] to enhance thermal performance. However, Hosseini et al. [31] conducted an experimental and numerical study comparing longitudinal and annular fins in a horizontal latent heat storage system. Results showed that longitudinal fins enhanced natural convection more effectively, achieving 17% (experimental) and 13% (numerical) better performance than annular fins. Liquid fraction contours further confirmed the faster and more uniform melting with longitudinal fins. Zhang et al. [32] reviewed different fin configurations, emphasizing that helical and topologically optimized fins show great research potential due to their superior performance compared to traditional shapes. In addition to conventional fins, some researchers have explored spiral or helical configurations. The helical geometry of spiral fins provides a continuous, extended surface area along the HTF tube, improving thermal contact with the PCM. This contrasts with annular or longitudinal fins, which create discrete thermal contact zones. Spiral fins maintain an uninterrupted PCM domain, promoting consistent energy distribution and avoiding the compartmentalization risked by annular fins. Several authors have researched the enhancement of thermal performance in phase change systems using spiral fins [33-45]. Although spiral fins require precise brazing, increasing manufacturing costs, this is offset by their long-term durability and performance gains.

Miao et al. [40] investigated the role of spiral fins in enhancing the solidification performance of latent heat thermal energy storage systems using paraffin wax as the PCM. Through numerical simulations, the study compares single, double, triple, and quadruple fin configurations while maintaining constant heat transfer surface area. Results show that triple fins provide the best balance, reducing solidification time by 24% compared to a single fin. Nie et al. [43] performed numerical investigation of vertical shell-tube latent heat storage unit using helm shaped fin to enhance the discharging rate. The helm-shaped fin consists of several annular parts and rectangular parts. Eighteen helm-shaped fins considering with different offsets of rectangular part, volume ratios, height ratios and thickness ratios were designed. For superior discharging performance, they claimed shorter annular part and longer rectangular part of helm shaped fin. Pizzolato et al. [44] demonstrated the use of topology optimization for heat transfer enhancement in Latent Heat Thermal Energy Storage tanks. We optimized the layout of a highly conductive material embedded in a phase change material to maximize the performance of the heat exchanger. Lv et al. [45] conducted a comparative analysis of the thermal performance of LHSUs with different fin geometries, further highlighting the advantages of these designs. The fins' shapes chosen in the present analysis were longitudinal, H-shaped, and spiral fins. They concluded that spiral fins performed best among other configurations for storing the energy during the

charging the process as that configuration stored energy of
567.35 MJ and mean power of LHSU 24.24 kW. According to the literature, no experimental study on a low-temperature application LHSU has been reported that investigates the improvement of the discharging rate in a shell-and-tube unit with different orientations using spiral fins. A lack of comprehensive experimental data quantifying the effect of spiral fins on the solidification process across different orientations exists. Furthermore, while orientation significantly influences melting behavior where natural convection dominates, its effect on the primarily conduction-dominated solidification process is not well-understood for finned systems. Therefore, this study aims to fill this gap by providing a systematic experimental evaluation of a spiral-finned LHSU, investigating its discharging performance in horizontal, vertical, and inclined orientations to determine the interplay between fin design and orientation.

2. METHODOLOGY

Figure 1 presents both a schematic diagram and photographic view of the experimental test setup used in this study. The core test section features a shell-and-tube heat exchanger constructed from two concentric tubes (60 mm in length). The inner brass tube has diameters of 28 mm (ID) and 30 mm (OD), while the outer stainless steel tube measures 88 mm (ID) and 92 mm (OD). To minimize heat losses, the outer tube is insulated with 2-3 layers of high-quality Cerawool. Water serves as the heat transfer fluid (HTF), circulating through the inner tube, while the annular space between tubes contains the phase change material (PCM) as a stearic acid with a melting point range of 55.7°C to 56.6°C. Stearic acid (fatty acid) possesses a melting temperature in this range and is easily available natural PCM. Moreover, Salunkhe and Krishna [46] and Alva et al. [47] reviewed PCM employed for solar water heating and space heating applications in which fatty acids and paraffin wax are mostly preferred for low temperature applications. During charging, hot water from a constant-temperature bath transfers thermal energy to melt the PCM. Conversely, during discharging, cold-water circulation promotes PCM solidification, releasing stored energy. Manual valves control both processes.

The inner tube is secured at both ends with threaded circular plates (Figure. 2). The LHSU's dimensions ensure complete PCM melting within 6-8 hours under typical HTF flow conditions. An adjustable mounting mechanism enables testing at various inclination angles (θ = 0°, 15°, 30°, 45°, 60°, 75°, and 90°). This experimental setup is specifically designed for low-temperature thermal applications.

The thermal properties of stearic acid, including its melting point and latent heat of fusion, were characterized using Differential Scanning Calorimetry (DSC), with results shown in Figure 3.

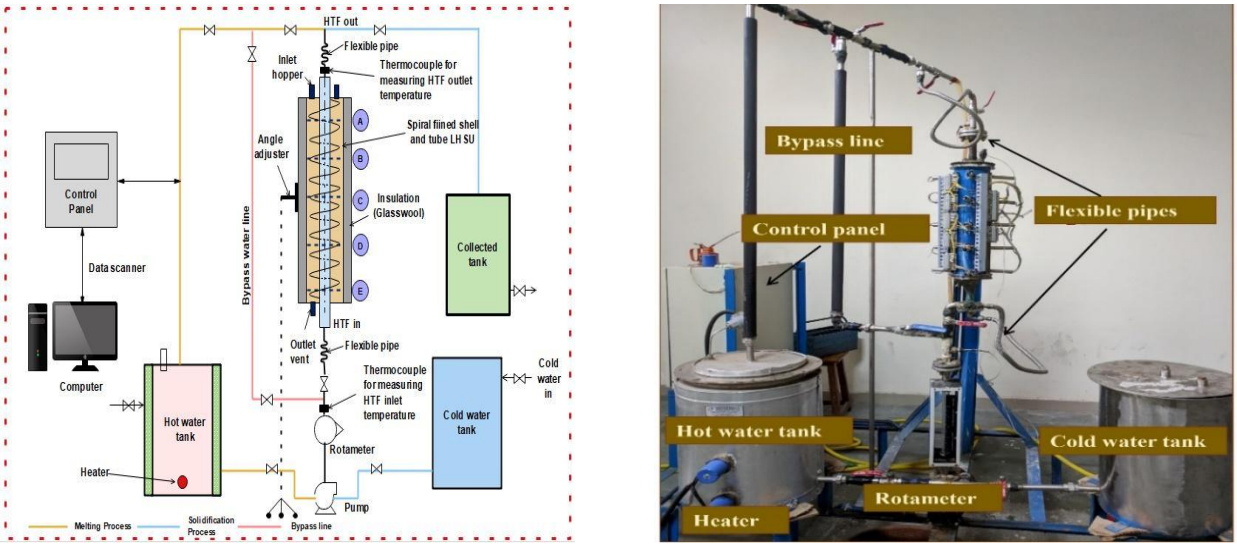

Figure 1. (a) Schematic of Shell and tube type LHSU (b) Picture of experimental test setup

Figure 2. Photograph of inner tube or HTF tube with a circular plate

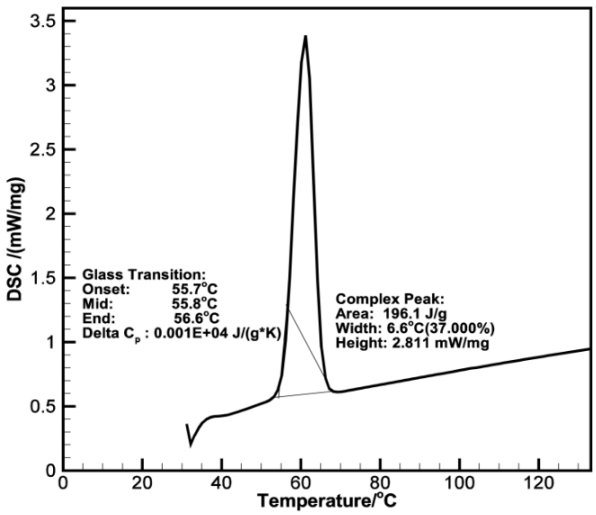

Figure 3 Measurement of latent heat and phase change temperature with DSC

Table 1 [48-50] summarizes the thermophysical properties of both stearic acid and water (the HTF). Prior to experimental testing, the system was calibrated by loading 2.5 kg of stearic acid into the shell-and-tube PCM container and conducting preliminary test runs. At the top of the LHSU, a smaller air gap is present to permit PCM thermal expansion during melting. Hot water from a bath maintained at a consistent temperature transfers energy to the PCM during the melting process. In the process of charging, the PCM melts and stores energy as heat. The water from the constant temperature cold bath is circulated through the test section. The PCM solidifies and releases the energy in the form of heat. The water at the exit of test section is at higher temperature. Flexible pipes are included at the HTF tube's intake and output to allow for various LHSU orientations.

Figure. 4 shows the geometrical details of spiral fins which is made of aluminum are brazed to the outer wall of the HTF pipe for enhancing the
charging and discharging process of the PCM. There are specific holes are provided on the outer shell of the test section so that thermocouples are inserted to measure the temperature of PCM near the HTF tube, at the middle and at the outer most position of the shell. Thus, the pitch of the spiral fins is chosen in such a way that thermocouples can be inserted easily from the outer shell and they can measure the temperature of the PCM between two successive fins. Further, as fins are required to be brazed on the test section thus the fins thickness is chosen to be 2.5 mm to ensure the sufficient strength of the fins. The geometric details of spiral fins are presented in Table 2.

2.1 Temperature measurement in LHSU

For accurate measurement of the temperature of the phase change material (PCM), 45 K-type thermocouples are installed within the annular space of the concentric tubes in the latent heat storage unit (LHSU), oriented vertically ($\theta = 90°$) as illustrated in Figure. 5. The thermocouples are distributed along five axial planes-designated as A, B, C, D, and E. At each axial plane, nine temperature probes are arranged in both radial and angular directions, with the angular positions spaced 120° apart. The temperature probes are arranged in sets based on their angular and radial positions within the annular space of the latent heat storage unit. Each set - (1, 4, 7), (2, 5, 8), and (3, 6, 9) - is spaced 120° apart in the angular direction to ensure uniform circumferential coverage. These probes are further distributed across three radial locations relative to the heat transfer fluid (HTF) pipe surface:

- Probes 1, 2, and 3 are located 1 mm from the HTF pipe surface, representing the inner radial zone closest to the heat source.
- Probes 4, 5, and 6 are positioned 15 mm from the HTF pipe surface, corresponding to the mid-radius region of the test unit.
- Probes 7, 8, and 9 are placed 28.5 mm from the HTF pipe surface, situated near the outer boundary of the test unit.

Table 1 Thermo-physical properties of PCM and HTF [48-50]

PCM	Melting point (°C)	Latent heat (kJ/kg)	Density (kg/m^3)		Specific heat (J/kg °C)		Thermal conductivity (W/m °C)		Coefficient of thermal expansion	Dynamic viscosity (kg/ms)
			Solid	Liquid	Solid	Liquid	Solid	Liquid		
Stearic acid	55.7-56.6	196.1	960	840	2860	2100	0.3	0.172	0.0001	0.00772
HTF			Density (kg/m^3)		Specific heat (J/kg °C)		Thermal conductivity (W/m °C)			
Water			997		4180		0.586			

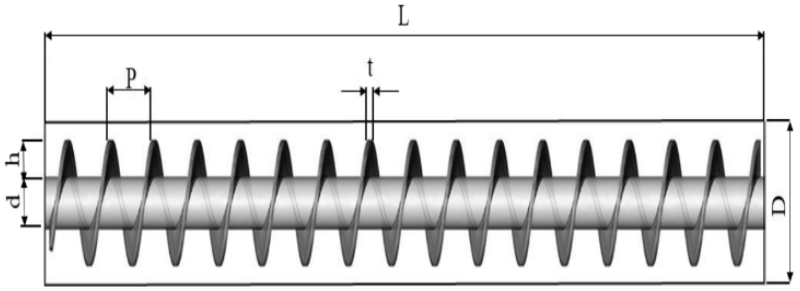

Figure 4 CAD model of Spiral fins with geometrical parameters

Table 2 Geometry details of spiral fins

Material	Thickness (mm)	Pitch (mm)	Height (mm)
Aluminium	2.5	37	20

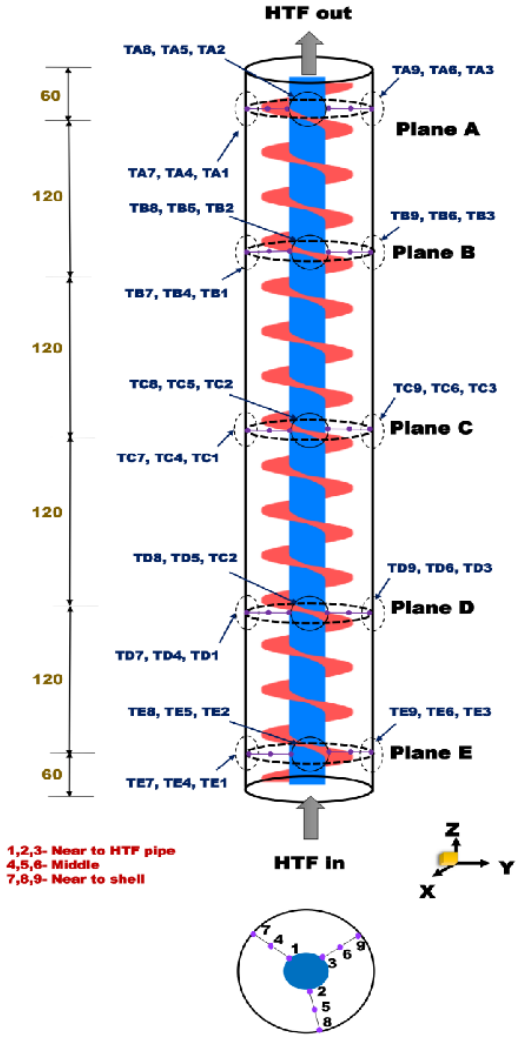

Figure 5 Positioning of different thermocouples in vertical LHSU

This spatial configuration allows for comprehensive temperature mapping in both radial and angular directions at multiple axial planes.

2.2 Uncertainty and repeatability of the system

The test rig consists of two measurement instruments i.e. thermocouples and rotameter. Uncertainty analysis in the present experimental study is based on the procedure suggested by Kline and McClintock [51]. There is a ±0.1°C uncertainty in temperature readings and a ±0.05 LPM uncertainty in the HTF mass flow rate. At HTF inlet temperature of 85ºC and mass flow rate of 5 LPM, the maximum percentage of uncertainty in the heat transfer corresponding to each orientation (θ = 90°, 45°, 0°) is estimated and tabulated as shown in Table 3. Repeatability of temperature measurement is ascertained by several test runs and simultaneous temperature measurements.

2.3 Experimental Procedure

Following is the experimental procedure for the present test setup.

A. Initial Setup & PCM Solidification

1. Fill the annular space with melted PCM.
2. Circulate cold water until the PCM is fully solidified.
3. Start the data acquisition software to record temperatures.

B. Charging (Melting) Process

4. Heat water in the hot bath to the desired initial temperature.
5. Set the hot water to the required flow rate (1-5 LPM).
6. Switch the flow path to pass hot water through the HTF pipe.
7. Continue until all PCM temperature probes indicate a steady state above the melting point.

C. Discharging (Solidification) Process

8. Switch the flow path to pass cold water at the same flow rate.
9. Continue until all PCM temperature probes indicate a steady state below the solidification point.

D. Data Collection & Repetition

10. Stop the program and save all recorded temperature data.
11. Repeat steps 4-10 for the next combination of flow rate and initial HTF temperature.

2.4 Estimation of retrieved energy

Energy storage rate is estimated by measuring HTF inlet and outlet temperature temperature sensors positioned at the upstream and downstream of the HTF pipe

Heat transfer (cumulative) between the HTF and PCM is estimated as:

$$Q_{m/s} = \int_0^{t_1} q\,dt + \int_{t_1}^{t_2} q\,dt + \ldots\ldots + \int_{n-1}^{t_n} q\,dt \qquad (1)$$

Where, q is the instantaneous heat transfer rate between HTF and PCM assuming no heat loss. It can be estimated as:

For melting/charging,

$$q_m = \dot{m}_f\, C_{pw}(T_{w,inlet} - T_{w,outlet}) \qquad (2)$$

For solidification/discharging,

$$q_s = \dot{m}_f\, C_{pw}(T_{w,outlet} - T_{w,inlet}) \qquad (3)$$

Table 3 Uncertainty in heat transfer (in percentage) for different orientations

Angle of inclination	Horizontal (θ = 0°) (in percentage)	Inclined (θ = 45°) (in percentage)	Vertical (θ = 90°) (in percentage)
	1.252	1.362	1.269

3. RESULTS AND DISCUSSION

The discharging process begins by circulating cold heat transfer fluid (HTF), specifically water, from a cold water tank. The temperature and flow rate of the HTF are maintained at 28 °C and 5 LPM, respectively. A comparative analysis of thermal performance with and without fins is conducted for three orientations of the latent heat storage unit (LHSU): vertical (θ = 90°), horizontal (θ = 0°), and inclined (θ = 45°). The comparison is based on the time required for the PCM to cool down to 35 °C. Additionally, the average PCM temperature and the retrieved energy rate are evaluated for each orientation.

The transient temperature profiles of the PCM at axial planes B and D, both with and without fins installed in the middle section of the vertical (θ = 90°) configuration, are presented in Figure. 6. Thermocouples located at plane B (TB4, TB6) and plane D (TD4, TD6) show a rapid temperature decrease, as illustrated in Figures. 6(a) and 6(b), reaching the PCM solidification point within 30 minutes. In contrast, for configurations with fins, the PCM and fin temperatures are initially higher at the start of the discharging process. As the cold HTF flows through the central pipe, the fins begin to cool down gradually, enhancing heat extraction from the surrounding PCM.

The PCM temperature near the HTF pipe drops more rapidly, leading to an earlier onset of phase change in this region. Notably, the inclusion of fins does not significantly enhance heat transfer until the PCM begins to solidify. Once solidification starts, however, the fins play a crucial role by reducing thermal resistance and improving thermal contact between the solidifying PCM and the cold surface. Between 50 and 130 minutes, a critical divergence in behaviour is observed. In the unfinned configuration (Figs. 6a and 6b), the temperature decrease is gradual as the process is hindered by the PCM's low thermal conductivity.

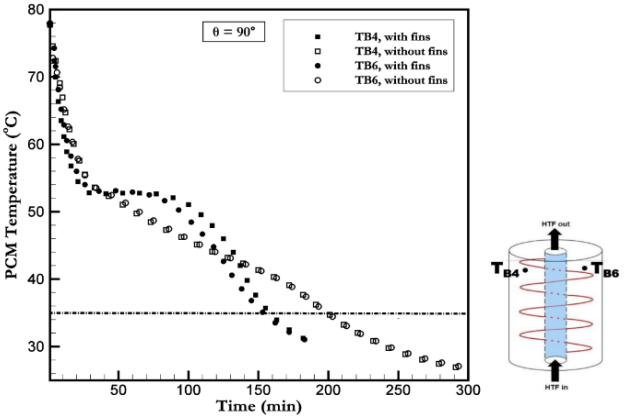

(a)

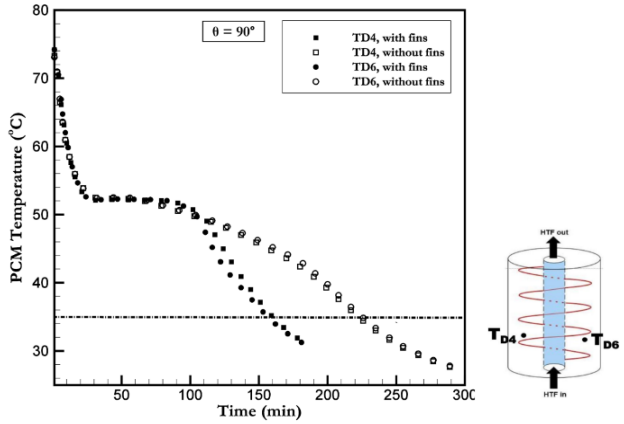

(b)

Figure 6. Comparison of axial temperature profiles during discharge for vertical (θ = 90°) LHSU configurations (finned vs. unfinned) at measurement planes B and D.

In contrast, the finned configuration exhibits a steeper temperature drop during this period. The spiral fins actively extract heat, creating a more pronounced temperature gradient and accelerating the progression of the solidification front.

As the PCM solidifies, its fluidity significantly decreases, effectively suppressing natural convection within the material. This means that the orientation, which primarily influences convective heat transfer, has a reduced role once the solidification front progresses and conduction becomes the prevailing mode of heat transfer. The presence of spiral fins further enhances this effect by providing direct pathways for heat conduction, reducing thermal resistance, and improving thermal contact between the solidifying PCM and the cold surface. This enhanced thermal connectivity promotes more efficient conduction heat transfer during the final stages of the discharging process. This enhanced thermal connectivity promotes more efficient conduction heat transfer during the final stages of the discharging process, as TB6 and TB4 reach to 35°C in 204 minutes for the case without fins whereas TD4 and TD6 reach to 35°C in 224 minutes (Figure. 6). The presence of spiral fins accelerates the discharging rate toward the end of the process compared to configurations without fins. For the case with fins, TB6 and TB4 reach to 35°C in 156 minutes whereas TD4 and TD6 reach to 35°C in 158 minutes. All four temperature probes reach to the desired temperature at the time interval. It is clear that no difference in the time required to approach the temperature of 35°C for the Plane B and Plane D thermocouples. However, the temperature at plane B (located in the upper axial region) decreases more quickly than at plane D. This can be attributed to the presence of an air gap, which facilitates PCM shrinkage during solidification. Additionally, the absence of noticeable angular temperature variation between TB4 and TB6 at plane B, and between TD4 and TD6 at plane D, suggests an axisymmetric temperature distribution and solid-liquid interface within the test section. Discharging time for TB4 and TB6 with fins are 23.53% for plane B conversely discharging time for TD4 and TD6 i.e. plane D has been reduced by 29.46%. Figure 7 illustrates the comparison of PCM temperature at axial planes B and D specifically at thermocouple positions TB4, TB6, TD4, and TD6 in the horizontal configuration of the LHSU. As shown in Figures 7(a) and 7(b), there is no noticeable difference in the time required to reach the solidification temperature at either axial location for both the cases with and without fins.

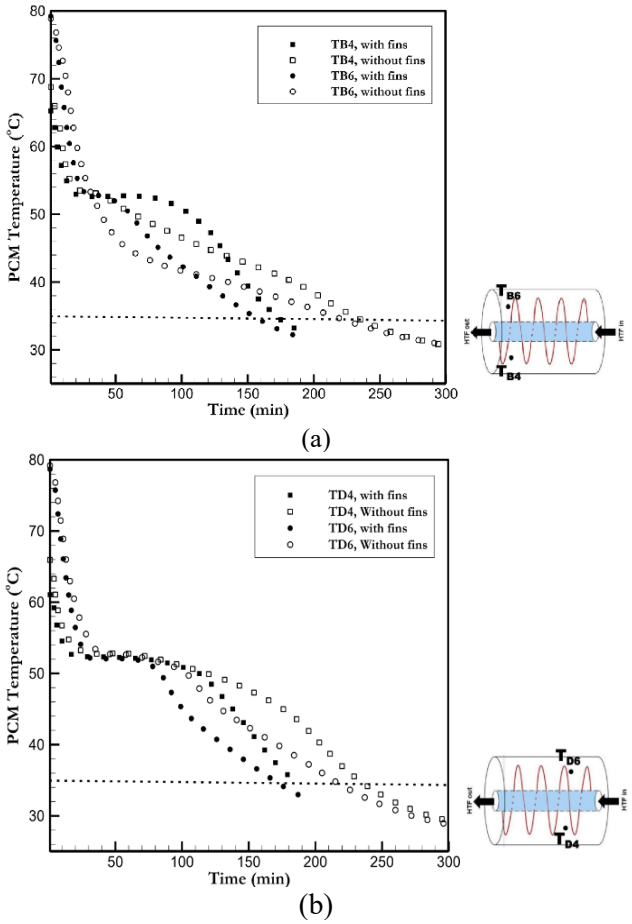

Figure 7. Comparison of axial temperature profiles during discharge for horizontal (θ = 0°) LHSU configurations (finned vs. unfinned) at measurement planes B and D

Observing the Figure. 7 (a) and Figure. 7(b) for the case without fins, TB4 and TB6 approach to the 35°C in 212 and 185 minutes respectively. Whreas for plane D, TD4 and TD6 reach to the 35°C in 233 and 213 minutes respectively. In the presence of fins, the reduction in their temperature facilitates thermal energy transfer during the later stages of discharging, thereby decreasing the overall solidification time. the TB4 and TB6 approach to the 35°C in 171 and 154 minutes respectively. Whereas for plane D, TD4 and TD6 reach to the 35°C in 182 and 168 minutes respectively. Consequently, due to the increased thermal contact area provided by the fins, the discharging time for TB4 was reduced by 19.3% and for TB6 by 16.8%, whereas for discharging time for TD4 was reduced by 21.9% and for TD6 by 21.1%

Figures 8(a) and 8(b) show the temporal variation of PCM temperature at different axial locations i.e. plane B (probes TB4 and TB6) and plane D (probes TD4 and TD6) - for the inclined orientation of the LHSU, with and without fin installation. As examined from Figure. 8, all four thermocouples reach the solidification temperature simultaneously, indicating a uniform solidification rate along the axial direction.

TB4 and TB6 advances to 35°C in 222 and 216 minutes whereas TD4 and TD6 reach to 262 minutes. With incorporation of fins, the discharging time for TB4 was reduced by 19.3% and for TB6 by 16.8%, whereas for discharging time for TD4 was reduced by 21.9% and for TD6 by 21.1%.

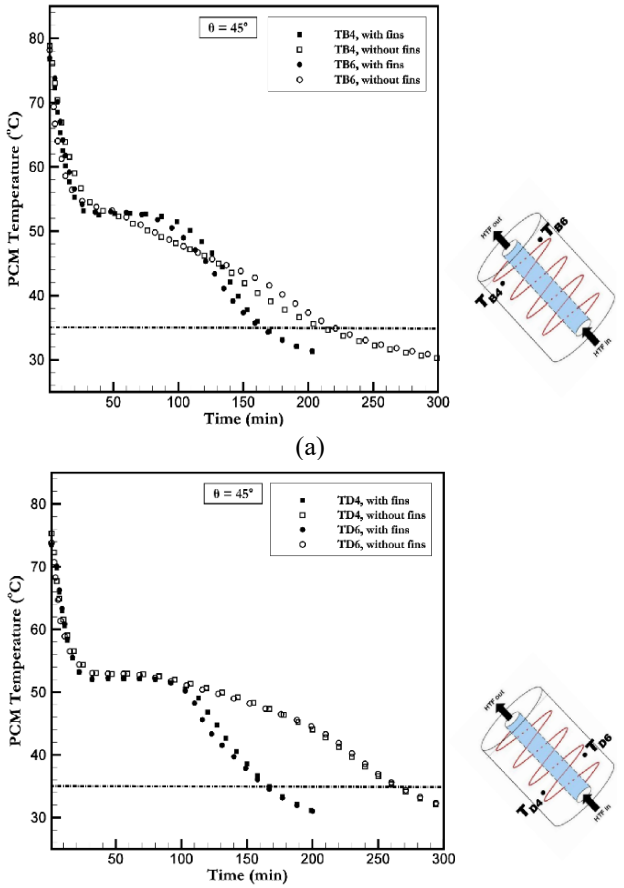

Figure 8. Comparison of axial temperature profiles during discharge for inclined (θ = 45°) LHSU configurations (finned vs. unfinned) at measurement planes B and D.

3.1 Comparison of PCM average temperature

The discharging performance of the spiral-finned LHSU was further examined by evaluating the temporal variation of the average PCM temperature and the corresponding energy retrieval rate for all three orientations, as shown in Figure 9. All experiments were carried out under identical conditions, with the cold HTF (water) supplied at an inlet temperature of 28 °C and a flow rate of 5 LPM. Figure 9(a) depicts the evolution of the average PCM temperature during solidification, calculated from the 45 thermocouples positioned within the annular region. The results reveal only minor differences among the vertical (θ = 90°), horizontal (θ = 0°), and inclined (θ = 45°) orientations. The average PCM temperature reached 35 °C in approximately 142, 154 and 152 minutes for the vertical, horizontal, and inclined configurations, respectively. These small deviations within about 8% of the shortest discharging time, indicate that orientation exerts only a negligible influence on the overall performance when spiral fins are employed.

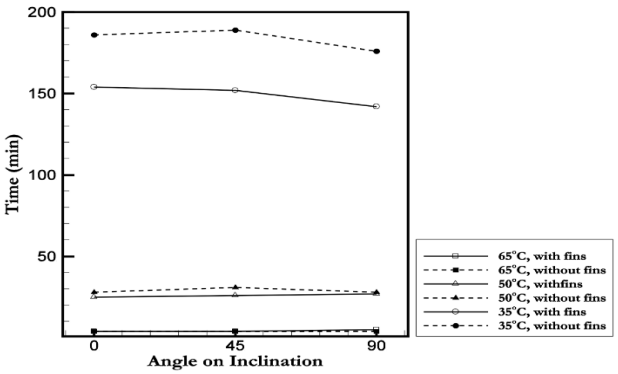

(a) Comparison of the average PCM temperature during discharging between vertical, horizontal and inclined LHSU

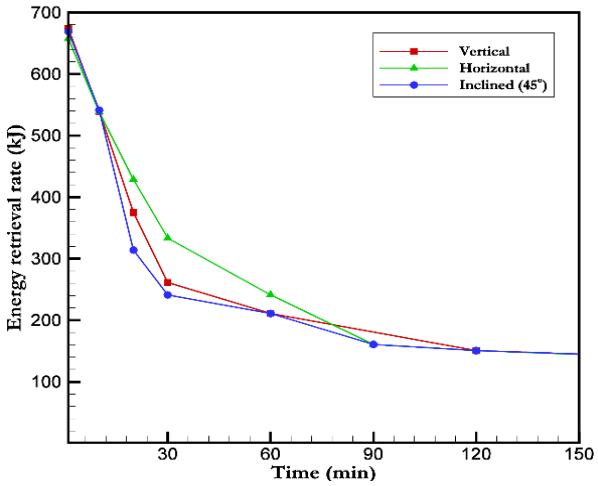

(b) Corresponding rate of energy retrieval over time.

Figure 9 Comparison of discharging performance for the finned LHSU across different orientations (a) comparison of PCM average temperature (b) energy retrieval rate.

Figure 9(b) illustrates the energy retrieval rate over time. During the initial 15–20 minutes, the retrieval rates are nearly identical for all orientations, reflecting the uniform conduction-dominated heat transfer promoted by the fins. Beyond this period, the horizontal configuration exhibits a slightly slower rate compared with the vertical and inclined cases. This behaviour can be attributed to the accumulation of a larger volume of liquid PCM above the HTF tube in the horizontal position, which slows the upward advance of the solidification front. In contrast, the vertical configuration enables a more symmetric progression of solidification around the tube, leading to marginally faster energy recovery.

This outcome can be explained by the dominant heat transfer mechanism during discharging. As the PCM solidifies, its mobility decreases drastically, suppressing natural convection and rendering

conduction the prevailing mode of heat transfer. Under these conditions, the effect of orientation, which primarily alters buoyancy-driven convection, becomes insignificant. The spiral fins provide continuous conductive pathways, effectively transferring heat from the PCM to the HTF tube in all directions. This uniform thermal connectivity mitigates orientation-dependent variations and ensures consistent performance.

The findings are further substantiated by the data in Table 4, which quantifies the influence of the fins on solidification time. In the middle section, the fins reduced discharging time by 26.5%, 25.96%, and 24.37% for the vertical, horizontal, and inclined orientations, respectively. For the entire annulus, the reductions were 19.3%, 17.2%, and 19.58%, respectively. The close agreement variations within 2.5 percentage points demonstrates that the enhancement achieved with spiral fins is essentially orientation independent.

Table 4 Comparison of time (minutes) required to attain average PCM temperature (to reach 35 °C) at the middle section and in the annulus between fins and without fins

In the Middle section (Average all 15 thermocouples)			
	Without fins (minutes)	**With fins (minutes)**	**Percentage reduction in discharging time**
Vertical (θ = 90º)	200	147	26.5
Horizontal (θ = 0º)	208	154	25.96
Inclined (θ = 45º)	197	149	24.37
In entire annulus (Average of 45 thermocouples)			
	Without fins (minutes)	**With fins (minutes)**	**Percentage reduction in discharging time**
Vertical (θ = 90º)	176	142	19.3
Horizontal (θ = 0º)	186	154	17.2
Inclined (θ = 45º)	198	152	19.58

4. CONCLUSION

This study presents a systematic experimental evaluation of the thermal performance of a Latent Heat Storage Unit (LHSU) in three orientations (θ = 0°, 45°, 90°). The setup incorporated 45 strategically positioned thermocouples within the PCM-filled annulus to capture three-dimensional temperature distributions. Measurements were recorded at five axial planes (A-E), with each plane containing nine thermocouples to monitor radial and angular (120° spacing) thermal gradients. Key findings include Spiral fins consistently improved discharging rates, reducing solidification time by 17.2-19.58% in the entire annulus and 24.37–26.5% compared to unfinned configurations, with no significant variation across orientations. Orientation effects were negligible due to the dominance of conduction during PCM solidification, which minimizes convective influences. The marginal differences observed (e.g., 1–2% variation in time reduction between vertical and horizontal configurations) fall within experimental uncertainty. Fins enhanced thermal connectivity by reducing interfacial resistance, accelerating energy retrieval uniformly in radial, axial, and angular directions.

The results underscore that spiral fins are orientation-agnostic, offering reliable performance enhancement for LHSUs in practical applications. Future work could explore fin geometry optimization to further reduce solidification time.

REFERENCES

[1] H. Mehling and L. F. Cabeza, “Phase change materials and their basic properties,” in Thermal Energy Storage for Sustainable Energy Consumption: Fundamentals, Case Studies and Design, Dordrecht: Springer Netherlands, 2007, pp. 257–277.

[2] K. Du, J. Calautit, Z. Wang, Y. Wu, and H. Liu, “A review of the applications of phase change materials in cooling, heating and power generation in different temperature ranges,” Appl. Energy, vol. 220, pp. 242–273, 2018.

[3] A. Sharma, V. V. Tyagi, C. R. Chen, and D. Buddhi, “Review on thermal energy storage with phase change materials and applications,” Renew. Sustain. Energy Rev., vol. 13, no. 2, pp. 318–345, 2009.

[4] S. Tomassetti et al., “Thermal properties of alternative phase change materials for solar thermal applications,” Int. J. Heat Technol., vol. 41, no. 3, 2023.

[5] C. Ding, J. Pei, S. Wang, and Y. Wang, “Evaluation and comparison of thermal performance of latent heat storage units with shell-and-tube, rectangular, and cylindrical configurations,” Appl. Therm. Eng., vol. 218, p. 119364, 2023.

[6] D. S. Mehta, K. Solanki, M. K. Rathod, and J. Banerjee, “Thermal performance of shell and tube latent heat storage

unit: Comparative assessment of horizontal and vertical orientation," J. Energy Storage, vol. 23, pp. 344–362, 2019.
[7] D. S. Mehta, K. Solanki, M. K. Rathod, and J. Banerjee, "Influence of orientation on thermal performance of shell and tube latent heat storage unit," Appl. Therm. Eng., vol. 157, p. 113719, 2019.
[8] A. M. S. Aljumaily, A. A. Mohammed, and S. J. Aljabair, "Effect of mass flow rate in a shell and tube heat exchanger of different inner tube geometries during solidification of phase change material," Diyala J. Eng. Sci., pp. 136–156, 2024.
[9] A. M. S. Aljumaily, A. A. Mohammed, and S. J. Aljabair, "Effect of inner tube shapes in a heat exchanger on a solidification of phase change material," SSRN 4427085.
[10] A. M. S. Aljumaily, A. A. M. Hayes Al-Jubouri, and N. F. H. Al-Jubouri, "Improving the thermal storage system (LHTES): A theoretical and experimental study," Int. J. Mech. Therm. Eng., vol. 5, no. 1, pp. 41–55, 2024.
[11] Y. B. Tao and Y. L. He, "A review of phase change material and performance enhancement method for latent heat storage system," Renew. Sustain. Energy Rev., vol. 93, pp. 245–259, 2018.
[12] B. Buonomo, O. Manca, S. Nardini, and R. E. Plomitallo, "Numerical study on phase change material with metal foam in shell and convergent/divergent tube thermal energy storage systems with external heat losses," Int. J. Heat Technol., vol. 42, no. 1, 2024.
[13] H. Niyas, C. R. C. Rao, and P. Muthukumar, "Performance investigation of a lab-scale latent heat storage prototype–experimental results," Solar Energy, vol. 155, pp. 971–984, 2017.
[14] L. Kalapala and J. K. Devanuri, "Effect of orientation on thermal performance of a latent heat storage system equipped with annular fins–an experimental and numerical investigation," Appl. Therm. Eng., vol. 183, p. 116244, 2021.
[15] L. Pu, S. Zhang, L. Xu, and Y. Li, "Thermal performance optimization and evaluation of a radial finned shell-and-tube latent heat thermal energy storage unit," Appl. Therm. Eng., vol. 166, p. 114753, 2020.
[16] X. Yang et al., "Thermal performance of a shell-and-tube latent heat thermal energy storage unit: Role of annular fins," Appl. Energy, vol. 202, pp. 558–570, 2017.
[17] L. L. Tian, X. Liu, S. Chen, and Z. G. Shen, "Effect of fin material on PCM melting in a rectangular enclosure," Appl. Therm. Eng., vol. 167, p. 114764, 2020.
[18] S. Tiari, A. Hockins, and K. Shank, "Experimental study of a latent heat thermal energy storage system assisted by varying annular fins," J. Energy Storage, vol. 55, p. 105603, 2022.
[19] S. Agrawal, P. M. Sutheesh, L. G. Kirankumar, and B. Rohinikumar, "Numerical investigations on thermal performance of latent heat thermal energy storage system with novel corrugated annular fins in PCM," J. Energy Storage, vol. 125, p. 116902, 2025.
[20] Y. K. Liu and Y. B. Tao, "Experimental and numerical investigation of longitudinal and annular finned latent heat thermal energy storage unit," Solar Energy, vol. 243, pp. 410–420, 2022.
[21] A. A. Al-Abidi et al., "Experimental study of melting and solidification of PCM in a triplex tube heat exchanger with fins," Energy Build., vol. 68, pp. 33–41, 2014.
[22] M. J. Hosseini, A. A. Ranjbar, M. Rahimi, and R. Bahrampoury, "Experimental and numerical evaluation of longitudinally finned latent heat storage systems," Energy Build., vol. 99, pp. 263–272, 2015.
[23] N. S. Dhaidan et al., "Experimental investigation of thermal characteristics of phase change material in finned heat exchangers," J. Energy Storage, vol. 71, p. 108162, 2023.
[24] M. K. Rathod and J. Banerjee, "Thermal performance enhancement of shell and tube latent heat storage unit using longitudinal fins," Appl. Therm. Eng., vol. 75, pp. 1084–1092, 2015.
[25] P. Wang et al., "Numerical investigation of PCM melting process in sleeve tube with internal fins," Energy Convers. Manag., vol. 110, pp. 428–435, 2016.
[26] M. Joybari, F. Haghighat, S. Seddegh, and A. A. Al-Abidi, "Heat transfer enhancement of phase change materials by fins under simultaneous charging and discharging," Energy Convers. Manag., vol. 152, pp. 136–156, 2017.
[27] M. Kazemi, M. J. Hosseini, A. A. Ranjbar, and R. Bahrampoury, "Improvement of longitudinal fins configuration in latent heat storage systems," Renew. Energy, vol. 116, pp. 447–457, 2018.
[28] C. Yu et al., "Melting performance enhancement of a latent heat storage unit using gradient fins," Int. J. Heat Mass Transf., vol. 150, p. 119330, 2020.
[29] D. S. Mehta, B. Vaghela, M. K. Rathod, and J. Banerjee, "Enrichment of heat transfer in a latent heat storage unit using longitudinal fins," Heat Transf., vol. 49, no. 5, pp. 2659–2685, 2020.
[30] L. A. Khan and M. M. Khan, "Role of orientation of fins in performance enhancement of a latent thermal energy storage unit," Appl. Therm. Eng., vol. 175, p. 115408, 2020.
[31] A. Hosseini, A. Banakar, S. Gorjian, and A. Jafari, "Experimental and numerical investigation of the melting behavior of a phase change material in a horizontal latent heat accumulator with longitudinal and annular fins," J. Energy Storage, vol. 82, p. 110563, 2024.
[32] S. Zhang, S. Mancin, and L. Pu, "A review and prospective of fin design to improve heat transfer performance of latent thermal energy storage," J. Energy Storage, vol. 62, p. 106825, 2023.
[33] A. Rozenfeld, Y. Kozak, T. Rozenfeld, and G. Ziskind, "Experimental demonstration, modeling and analysis of a novel latent-heat thermal energy storage unit with a helical fin," Int. J. Heat Mass Transf., vol. 110, pp. 692–709, 2017.
[34] D. S. Mehta, B. Vaghela, M. K. Rathod, and J. Banerjee, "Thermal performance augmentation in latent heat storage unit using spiral fin: an experimental analysis," J. Energy Storage, vol. 31, p. 101776, 2020.
[35] D. S. Mehta et al., "Heat transfer enhancement using spiral fins in different orientations of latent heat storage unit," Int. J. Therm. Sci., vol. 169, p. 107060, 2021.
[36] X. Sun et al., "Solidification enhancement in a triple-tube latent heat energy storage system using twisted fins," Energies, vol. 14, no. 21, p. 7179, 2021.
[37] S. A. Zonouzi and A. Dadvar, "Numerical investigation of using helical fins for the enhancement of the charging process of a latent heat thermal energy storage system," J. Energy Storage, vol. 49, p. 104157, 2022.
[38] K. Guedri et al., "Solidification acceleration of phase change material in a horizontal latent heat thermal energy storage system by using spiral fins," Case Stud. Therm. Eng., vol. 48, p. 103157, 2023.
[39] H. Li, C. Hu, D. Tang, and Z. Rao, "Improving heat storage performance of shell-and-tube unit by using structural-optimized spiral fins," J. Energy Storage, vol. 79, p. 110212, 2024.
[40] X. Miao et al., "Performance enhancement of latent heat thermal energy storage system by using spiral fins in phase change material solidification process," Process Saf. Environ. Prot., vol. 176, pp. 568–579, 2023.

[41] F. He, C. Hu, W. Gao, S. Li, and X. Meng, "Effect of inclination angles on heat transfer characteristics of solid and perforated spiral finned heat exchangers," Int. Commun. Heat Mass Transf., vol. 164, p. 108920, 2025.
[42] L. Bo et al., "Twisted-fin parametric study to enhance the solidification performance of phase-change material in a shell-and-tube latent heat thermal energy storage system," J. Comput. Des. Eng., vol. 9, no. 6, pp. 2297–2313, 2022.
[43] C. Nie, X. Liu, Z. Rao, and J. Liu, "Discharging performance evaluation and optimization of a latent heat thermal energy storage unit with helm-shaped fin," Appl. Therm. Eng., vol. 236, p. 121595, 2024.
[44] A. Pizzolato, A. Sharma, K. Maute, A. Sciacovelli, and V. Verda, "Design of effective fins for fast PCM melting and solidification in shell-and-tube latent heat thermal energy storage through topology optimization," Appl. Energy, vol. 208, pp. 210–227, 2017.
[45] L. Lv et al., "Experimental study on a pilot-scale medium-temperature latent heat storage system with various fins," Renew. Energy, vol. 205, pp. 499–508, 2023.
[46] P. B. Salunkhe, "Investigations on latent heat storage materials for solar water and space heating applications," J. Energy Storage, vol. 12, pp. 243–260, 2017.
[47] G. Alva, L. Liu, X. Huang, and G. Fang, "Thermal energy storage materials and systems for solar energy applications," Renew. Sustain. Energy Rev., vol. 68, pp. 693–706, 2017.
[48] M. R. Reddigari, N. Nallusamy, A. P. Bappala, and H. R. Konireddy, "Thermal energy storage system using phase change materials - Constant heat source," Thermal Sci., vol. 16, pp. 1097–1104, 2012.
[49] R. S. Kumar and D. J. Krishna, "Differential scanning calorimetry (DSC) analysis of latent heat storage materials for low temperature (40–80°C) solar heating applications," Int. J. Eng. Res. Technol., vol. 2, no. 8, pp. 429–455, 2013.
[50] K. Kant, A. Shukla, and A. Sharma, "Performance evaluation of fatty acids as phase change material for thermal energy storage," J. Energy Storage, vol. 6, pp. 153–162, 2016.
[51] S. J. Kline and F. A. McClintock, "Describing uncertainties in single sample experiments," Mech. Eng., vol. 75, 1953.